ADVANCES IN SLS POWDER CHARACTERIZATION

A. Amado*, M. Schmid†, G. Levy† and K. Wegener*

*Department of Mechanical and Process Engineering, Swiss Institute of Technology, Zurich 8008, Switzerland
†inspire AG, irpd Institute, St. Gallen 9014, Switzerland

Abstract

This paper introduces a new Selective Laser Sintering (SLS) powder characterization methodology. A better understanding regarding powder flow processing range is targeted. Intrinsic properties of polymers are given from the basic chemical structure and non-intrinsic ones describe characteristics caused from pre-processing and production. The non-intrinsic ones are dedicated to the powder. Understanding the particle size distribution and shape coupled with its ability to flow under the particular SLS processing conditions is desired. In this direction, a system called Revolution Powder Analyzer is employed and the dynamic powder behavior is characterized in nearly roll spreading conditions. This allows a sensitive differentiation of powders regarding their flow-ability and predicts, to a certain extent, the behavior under SLS conditions.

1 Introduction

1.1 *SLS Powder Development: State of the art*

The development of new powdered materials suitable for the Selective Laser Sintering Process with the aim to broaden its application field constitutes one of the main research topics and challenges nowadays [1,2,3,4]. The types of materials actually used are mostly neat polymers, particularly polyamides or polyamide based compounds [5], achieving a market share of 95% [3]. Several research efforts have being conducted during the last years towards the design of new SLS powders (see Table 1). In this direction, different approaches have been adopted, considering just from a simple mixture of two polymer components to more sophisticated production methods like mechano-chemical alloying [6,8]. Depending on the production method employed, intrinsic property changes can be induced, such as a shift of the melting or crystallization point. However, non-intrinsic features like the particles size and shape or powder flowability are strongly influenced in a sensitive way [9]. Regarding the materials characterization for its SLS process suitability, most researchers concentrate their effort on intrinsic properties (Table 1). Thermal and rheological measurements conducted by differential scanning calorimetry (DSC), termo-gravimetric analysis (TG), melt flow index evaluation (MFI) and rheometer testing methods (viscosity characterization) constitute a standard practice. However, non-intrinsic properties are normally barely reported or simple left out. It is well known that good dispersion conditions are necessary to achieve a higher powder packing and a homogeneous layer spreading, but no quantitative information towards a prediction for SLS powders is available in literature. Most researchers conduct a powder development cycle just by trial and error carried out on a full or scale SLS equipment. Salmoria et al. [7] investigated the processing of blends of commercial polyamide 12 (PA12) and high density polyethylene (HDPE) powders. A year later, a similar approach was performed, considering blends of polyamide 6

(PA6) and PA12 [10]. Sintered parts with high porosity were obtained and a powder pre-treatment is mentioned to improve the particle regularity. However, no clear information regarding particle size distribution (PSD) or shape was reported, which does not clearly allow distinguishing between a predominant intrinsic or non-intrinsic effect. Schultz et al. [8] investigated PA12-PEEK blends formed by cryogenic mechanical alloying. In this case, due the processing method employed, a flake-like structure of the alloyed particle is reported and a large amount of fines are revealed by the PSD analysis. The author attributes the lower mechanical properties to the difficulties in achieving a dense powder bed despite having achieved a good miscibility between both materials. More recently, the modification of polyamide with organic and inorganic nano-fillers to enhance polymer performance, i.e., fire retardancy, high strength and high heat resistance has been employed. Koo et al. [11] examined polyamide 11 and 12 modified with different types of nanoparticles produced by a twin extruder followed by a cryogenically grinding step. The subsequent trial and error cycle proved that not all blends were successful. The author states that the reason for the failure was the process inhibition by powder mechanics. The poor powder flow led to poor powder deposition and subsequent SLS processing difficulties. Even the rejected material is described as flour like flowing powder, but again a qualitative appraisal was elucidated.

Production Technology	Intrinsic characterization test				Non-intrinsic characterization test				Author/ Research Group
	DSC	TG	MFI/ Rheo.	*Others	PSD	Particle Shape	Tap/Bulk Density	**Others	
Powder mixing (polymer, fiber, beads)	✓	✗	✗	✓	✗	✗	✗	✗	[7][10][12]
	✗	✗	✗	✓	✗	✗	✗	✗	[13][14][15][16]
	✓	✗	✓	✓	✗	✗	✗	✗	[17]
Melt mixing & cryogenic grinding/spray drying	✓	✗	✓	✓	✓	✗	✗	✗	[18]
	✓	✗	✓	✓	✗	✗	✗	✗	[19]
	✓	✓	✓	✓	✓	✗	✗	✗	[11][20]
Dissolution-precipitation	✓	✓	✗	✓	✓	✗	✗	✗	[21]
	✓	✓	✓	✓	✓	✗	✗	✗	[22]
	✓	✓	✓	✓	✓	✗	✗	✗	[23]
Mechano-chemical alloying/ Solid state	✗	✗	✗	✓	✓	✗	✓	✓	[6][8]
	✓	✗	✓	✓	✓	✗	✓	✗	[9]
	✓	✗	✗	✓	✓	✗	✗	✗	[24]

Other characterization methods: *FTIR, EDX, XRD, etc.; **Angle Of Repose, Carr Index, etc.

Table 1: Material characterization methods employed by different authors

Table 1 summarizes for different authors/research groups the diverse production technologies employed and the materials characterization methods used prior and after carrying out the sintering trials. As noted, most of them did not consider any kind of powder flowability evaluation despite that each production process has a considerable different effect on the non-intrinsic powder properties. Normally just the particle shape characteristic is reported as irregular. Actually, there is no quantitative measurement technique in the existing SLS field to characterize the powder flow behaviour. This makes it very difficult to predict the process-ability of a new material a priori. Thus, it is suggested that a quantitative powder mechanics characterization methodology must be developed to facilitate the SLS processing [11].

1.2 *Non-intrinsic powder characterization*

The flow properties depend on many parameters, e.g., particle size distribution, particle shape, inter-particle forces, moisture and temperature [25]. It is a challenging task to determine theoretically the flow behaviour of bulk solids in dependence of all of these parameters. Thus it is necessary to determine the flow properties in appropriate testing devices. Evans et al. [26] introduced a "SLS Materials Development Method" were he emphasizes the importance of considering the powder behaviour as a first step on a powder development cycle. However, currently no specific method has been established. Many characterization techniques are available to determine the flow properties of powders. Krantz et al. [27] provide a comprehensive description of different techniques, considering static and dynamic powder state conditions. Table 2 gives an overview of the most common techniques in use, particularly in the food and pharmaceutical industry.

	Bed Expansion Ratio	Angle of Repose	Ring Shear Cell	Bulk/Tap Density
Method				
Measurement Condition	Dynamic under vertical fluid drag load	Static under free external load	Quasi-Static under pressure	Static under the effect of powder weight
Characterization parameters	Fluidized height v/s upstream fluid flow	Pile angle	Shear force v/s normal pressure/ compression rate	Loose and packed height v/s n° of taps
Standard	Not standardized	DIN ISO 4324	ASTM D6773	ASTM D7481

Table 2: Most common powder characterization methods [27]

It was established that results provided by each method are strongly dependent upon the powder stress condition. Therefore, techniques that consider an aerated state as the bed expansion ratio are appropriate to predict the fluidization performance, while externally loaded powder methods give an indication about static stability and compressibility ratio. Thus, no single technique is suitable for the full characterization of a powder and all of them, in principle, complement themselves. While more information is known about the handling system, the more likely it is to choose an accurate measurement device. Here must be emphasized to select a suitable characterization method that can replicate as closely as possible the boundary condition requirements. Unfortunately this is possible just for simple powder handling systems and geometries. For the SLS spreading system, a rather difficult appraisal about the deposition conditions can be assessed since no clear information is available to estimate if the stress state is next to a fluidized or a more compacted stress state.

2 Objective

The aim of this paper is to introduce a new powder characterization method into the SLS field that gives information regarding the dynamic behavior under a similar stress state when powder is spread over the part bed. The intent is not to replace traditional methods, but complement those existent to achieve a more accurate understanding about SLS powder suitability and thus reduce the powder development cycle time.

3 Experimental Device & Methodology

3.1 *Dynamic Powder System: Operational Principle*

The measurement device employed consists of a Revolution Powder Analyzer manufactured by Mercury Scientific Inc. It consists of a rotating and an image acquisition system as shown in Figure 1. The rotating drum is machined in aluminum with an inner diameter of 50 mm and 35 mm width. The lateral sides are covered with transparent glass, to allow the powder behavior inside be captured by the image acquisition system. The drum can be rotated at different speeds ranging from 0 to 200 rpm.

Figure 1: Schematic diagram of rotating and image acquisition system

With the aid of a backlight source, the powder free surface and cross sectional area of powder inside the drum can be recorded. Depending on the turning speed, two different tests can be performed: At low values, a discrete behavior is achieved based on a sequence of avalanches; at higher speeds, a continuous operation mode is reached, characterized by a steady state regime. The tested behavior is called *Flowability* and *Fluidization* respectively. For the present research, the initial set up and the different parameters employed for each method are summarized in the following table:

Flowability Test		Fluidization Test	
Parameter	**Value**	**Parameter**	**Value**
Sample Volume	25 cc (tap density)	Sample Volume	25 cc (tap density)
Rotating Speed	0,6 rpm	Prep. Rotating Speed	90 rpm
Preparation Time	30 s	Preparation Time	30 s
Avalanche Threshold	0,65 %	Initial Rotating Speed	50 rpm
Angle Calculation	Half	Final Rotating Speed	90 rpm
N° Avalanches to record	128	Rotating speed increment	10 rpm
Image capturing rate	15 fps	Image capturing rate	30 fps

*Internal drum surface roughness: Ra=2.6 μm
Table 3: Flowability and Fluidization test set up main parameters (RH: 40%; Room T°: 25 °C)

It must be pointed out that the drum rotational speed range for the Fluidization test can be adjusted to similar angular speeds of the translating roller during the powder deposition cycle (e.g., 35 to 80 rpm at a translational speed of 77 to 177 mm/s for a 3DSystems Sinterstation 2000 machine equipped with a 50 mm roller diameter).

It is important to remark that with this method a nearly similar stress state condition can be achieved in comparison to the techniques presented previously (Table 2). The boundary conditions generated for the powder surface inside the drum permit emulate the typical front stress free turning powder wedge behaviour generated by any of the actual SLS spreading systems, i.e., the counter-clockwise rotating roller (3DSystems) or the concave blade coater (EOS) (Figure 2).
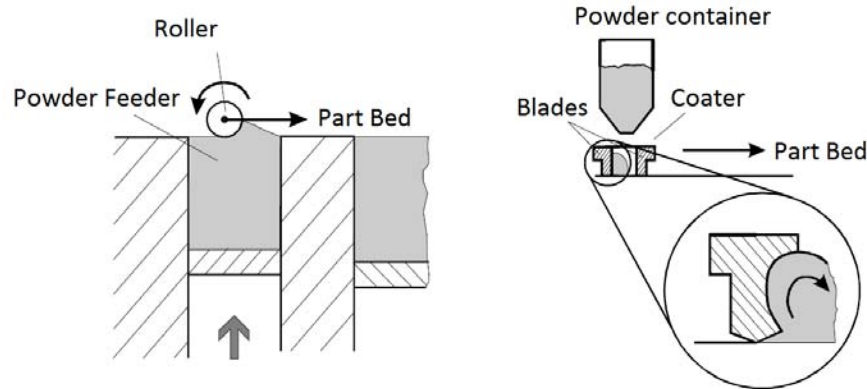
Figure 2: SLS powder spreading systems: Roller (3DSystems) & Blade (EOS) [28]

3.2 *Characterization Indexes*

Based on the sequence of images captured by the acquisition system, the following characterization parameters for each image are developed according to the specific test performed:

Avalanche Angle: corresponds to the angle obtained from a linear regression of the free surface at the maximum potential energy prior to the start of the powder avalanche occurrence. Normally the left half of the diameter is considered to obtain a more representative measure. As a general rule, the higher the avalanche angle the poorer the flowability. In comparison to the angle of repose presented previously in Table 2 (DIN ISO 4324), a distribution of values is obtained.

Surface Fractal: corresponds to the fractal dimension D of the free surface of the powder and provides an indication of how rough the powder surface is. The determination of this dimensionless parameter is based on the method used by Richardson [29] who proposed the empirical relationship relating the length estimate, $L(\varepsilon)$, with the scale, ε, of measurement given by:

$$L(\varepsilon) = M \, \varepsilon^{(1-D)}$$

where M is a positive value and D is a constant at least equal to unity. In our study the length estimate is related to the powder surface length and the scale ε is varied between a minimum limit that is defined by the image resolution (i.e., the pixel size) and a maximum that normally corresponds to one third of the drum diameter.
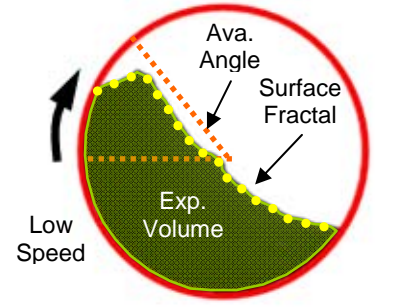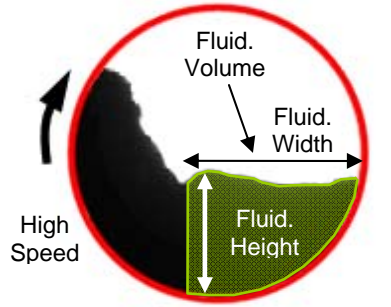
Flowability Test	Fluidization Test
Avalanche Angle	Fluidized Volume Slope
Surface Fractal	Fluidized Height Slope
Volume Expansion Ratio	Final Settling Time

Table 4: Flowability & Fluidization Indexes

The measurement is performed after each avalanche to determine how the powder reorganizes itself. If the powder forms a smooth even surface, the surface fractal will be near one. If the surface is rough and jagged, the surface fractal will be greater than one.

Volume Expansion Ratio (VER): corresponds to the ratio between the volume measured inside the drum (expanded volume that relates to the bulk density) and the volume occupied by the powder in the sample container before filling the drum during the preparation stage (tap density). The preparation step consists of filling a 25 cc cylinder under manual tapping until the maximum powder compaction is achieved. Then the upper surface of the cylinder is scraped out to accurately define a fixed volume for all samples. The expanded volume is measured as the sum of the area of every image pixel occupied by the powder multiplied by the width of the drum.

Fluidized Volume Slope: is defined as a linear regression analysis of the cumulative volume that is fluidized versus the angular velocity of the sample during the fluidization testing. The fluidized volume corresponds to the cross sectional area inside the drum which develops a near horizontal powder surface. The limit of this area is set when a high steep change of the free surface slope is generated (see Table 4).

Fluidized Height Slope: is defined as a linear regression analysis of the cumulative height of the fluidized volume versus the angular velocity of the sample during the fluidization testing.

Final Settling Time: corresponds to the time elapsed until the sample stops settling from the moment the drum rotation is stopped at the maximum rotational rate. In this case the powder settling corresponds to the reduction of the fluidized height versus time.

Also, for each powder tested, 3 consecutive measurements were considered, to determine any possible variations regarding the repeatability of the results.

Among the parameters presented, the ratio between the volume expanded and the sample volume (VER) can be correlated to a certain extent to the so called Hausner Ratio (HR) or Carr index $(CI=1-HR^{-1})$ (ASTM D7481) derived from compressibility studies. Both indexes are well accepted due to their relative ease of determination and excellent reproducibility in comparison to other indicators like the angle of repose (DIN ISO 4324). However, regardless of their wide applicability, they present some drawbacks [30]. Usually similar materials are not likely to be well differentiated. In fact, two materials with different bulk and tap densities but similar HR values are likely to behave very differently in practice [31]. Thus, a deeper understanding and adaptation towards specific applications like SLS are needed.

4 Results & Analysis

A selection of different SLS commercial polymer based materials and others under current research were tested with the aim to characterize their properties in relation to the indexes presented in the previous chapter. Powders under development, due a non-disclosure agreement, are labelled as Materials 1, 2A and 2B. The difference between A and B is a post-processing Spray Drying treatment to improve the particle shape (B). Table 5 provides a summary of the materials chosen and their principal features, including a PSD analysis on a volume basis considering an equivalent circular diameter.

Material	DF PA12	PA 2200	Alumide	DF HST	DF Flex	icoPP	Material 1	Material 2A	Material 2B
Base Material	PA 12	PA 12	PA 12	PA 12	TPE*	coPP	PA	PA	PA
Filler	None	None	Aluminium	Mineral Fibers	N/A	None	None	Nano-Silica	Nano Silica
Compound Method	Neat Polymer	Neat Polymer	Mech. Mixing	Mech. Mixing	Neat Material	Neat Polymer	Neat Polymer	Mechano Fusion	Spray Drying
Final Compound	1 Phase	1 Phase	2 Phases	2 Phases	1 Phase	1 Phase	1 Phase	1 Phase	1 Phase
PSD (μm)	D10=44 D50=56 D90=76	D10=39 D50=53 D90=72	D10=40 D50=65 D90=85	Not defined**	D10=64 D50=88 D90=98	D10=36 D50=58 D90=88	D10=40 D50=48 D90=65	D10=45 D50=97 D90=115	D10=22 D50=44 D90=70

* Thermoplastic Elastomer; ** Not representative results for PSD with high different aspect ratios

Table 5: SLS material properties tested with Revolution Powder Analyzer

For each material both proposed tests were performed considering the configuration previously described in Table 3. This set of materials was selected because it represents diverse compounding and mixing methods to obtain powders with heterogeneous and homogeneous mixed phases. Additionally PA12 based materials constitute at least 90% of the market share. Figure 3 depicts a sample image of each powder tested (same scale for all pictures).
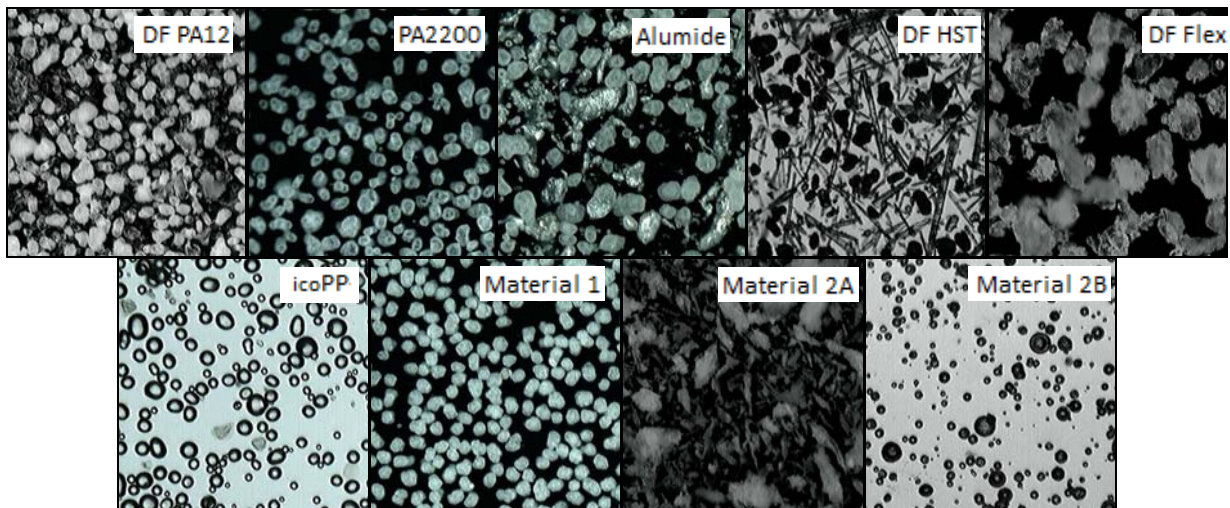

Figure 3: Image sample of SLS powders tested

The Flowability and Fluidization results are presented as follows:

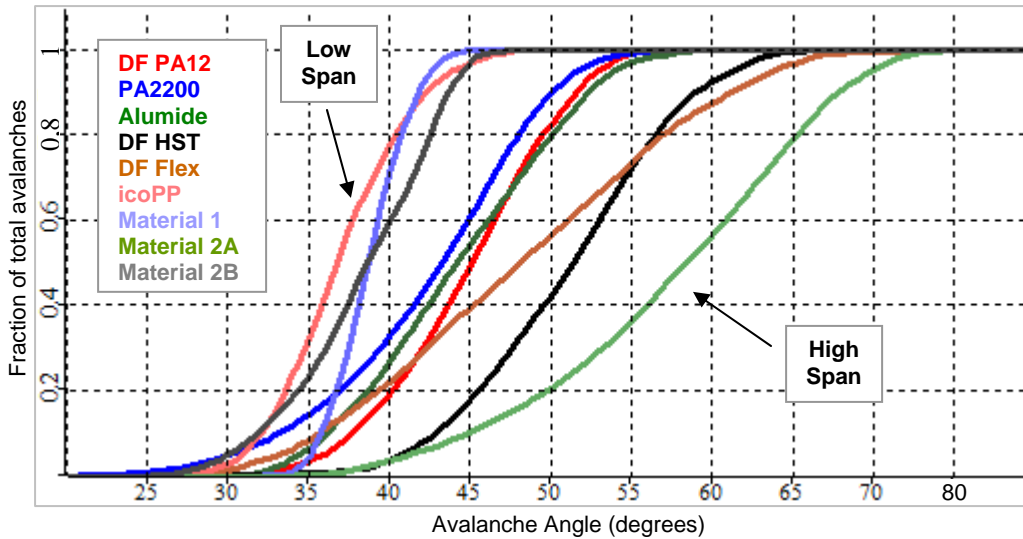## 4.1 Flowability Results

Figure 4: Cumulative Avalanche Angle Distribution

Figure 4 depicts the cumulative avalanche angle distribution for each material. As noted, different materials present different median values and also different curve symmetries (skewness). A low median angle coupled with a narrow value distribution (span) is correlated to a good flowing powder. In this case, icoPP, Material 1 and Material 2B present the lowest average D50 of 38°. These three powders present in common a fine PSD with a very near spherical shape and the presence of 1 phase. Following this characterization, DF PA12, PA2200 and Alumide constitute a second group with similar results. The average avalanche angle D50 achieves a value of 44° and these powders present a higher distribution of shapes with convex structures on its surface in comparison to the previous group (no relevant differences between 1 or 2 material phases). Finally, particles with a less geometrical defined shape or compounds with different shape aspect ratios, i.e., fibers or more complicated geometries like flakes can be grouped in a set of materials that present the highest avalanche angle and broader curve distributions. In this case, a trend is difficult to assess due the heterogeneity of the materials (DF HST, DF Flex and Material 2A).
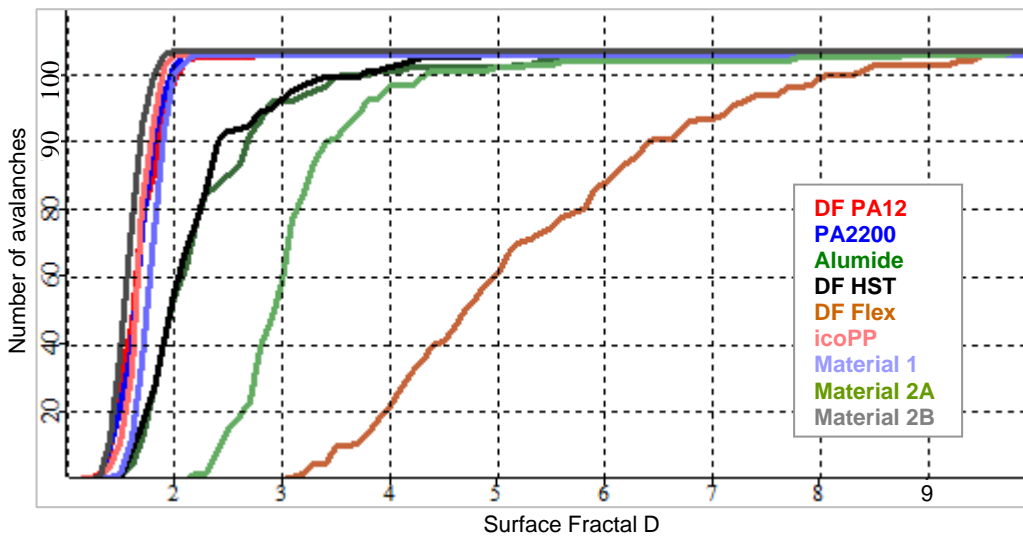

Figure 5: Cumulative Surface Fractal Distribution

The surface fractal results are depicted in Figure 5. In this case, in comparison to the avalanche distribution behaviour, this index does not distinguish between near spherical or broader shape distribution based powders, which can be grouped together with an average fractal dimension D50 of 1.72 (DF PA12, PA2200, icoPP, Material 1 and Material 2B). However, a second set of powders constituted by compounds with two heterogeneous phases, namely a polymeric matrix and filler, i.e., Alumide and HST, can be clearly differentiated with an average D50 value of 2.3. Concerning a correlation to the SLS spreading process, these results indicate that the free boundary generated after the avalanche for this second group presents a more structured or jagged surface that can influence the packing of the powder. Extreme distorted particle geometries like of Material 2A and DF Flex present clearly higher fractal values and thus, a lower packing.
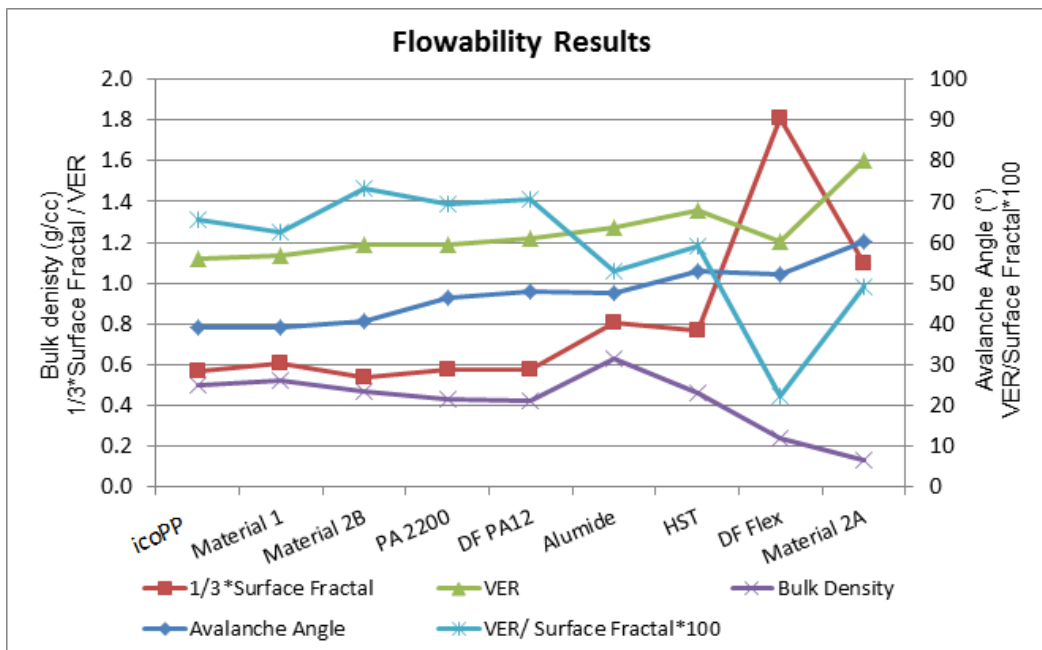

Figure 6: Summary of results for Flowability Indexes

Figure 6 summarises the results presented above for the median value of each index. Additionally, the volume expansion ratio (VER) is included and the bulk density of each powder measured inside the rotating drum. As observed, two main trends can be established. First, as the avalanche angle increases, the VER increases as well. This is in accordance with other results described in the literature. This VER indicator, due its definition, can be correlated to the so called Hauser Ratio described previously, which relates the tap and the bulk density of a powder. However, this index fails to describe accurately the behaviour of DF Flex. Concerning the VER (HR) classification, DF PA12 and DF Flex should present the same ability to flow, which disagrees with the empirical evidence (optimal processing conditions on 3DSystems equipment are completely different from DF PA12 to avoid streaking on the powder bed). Second, in general, an opposed effect between bulk density and avalanche angle can be observed. As the bulk density decreases, the avalanche angle increases. In case of Material 2A, despite having a lower density and higher VER in comparison to DF Flex, it presents a considerable lower surface fractal dimension. Therefore, both trends do not allow ranking adequately by themselves the powders under study in relation to a proper packing performance. Thus, based on the results

presented, a new indicator is proposed, based on the ratio between the VER and the Surface Fractal Dimension, i.e.:

$$Rank_{Index} = VER/D$$

As depicted in Figure 6, this index can better rank the powders regarding its SLS suitability. The higher score is obtained for Material 2B (spray dried) and the two commercial PA12 in agreement with the empirical experience on SLS equipment and their ease of processing. Materials icoPP and Material 1 can be classified below the neat polyamides and finally, both filled materials with a heterogeneous phase, i.e. Alumide and DF HST follow in this classification. Finally, DF Flex results to be the lowest ranked material followed by the flake like powder Material 2A. In general, the author propose that this index constitutes an improved description due its ability to couple information regarding the pile stability and powder rearrangement, which can better explain how DF PA12 and PA2200 fulfil an adequate compromise between these two factors.

4.2 *Fluidization Results*

Regarding the test at higher rotational speeds, the results for the fluidized powder height and volume are depicted in Figure 7 & 8.
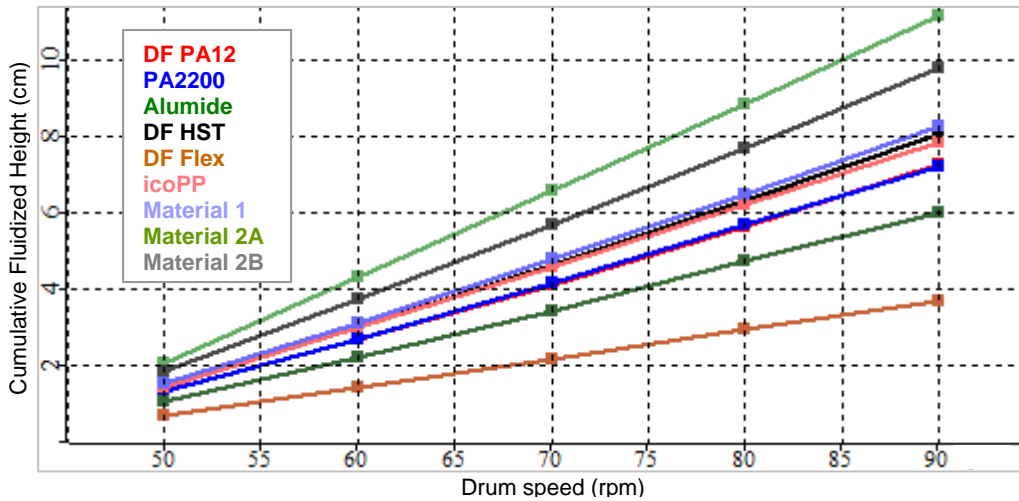

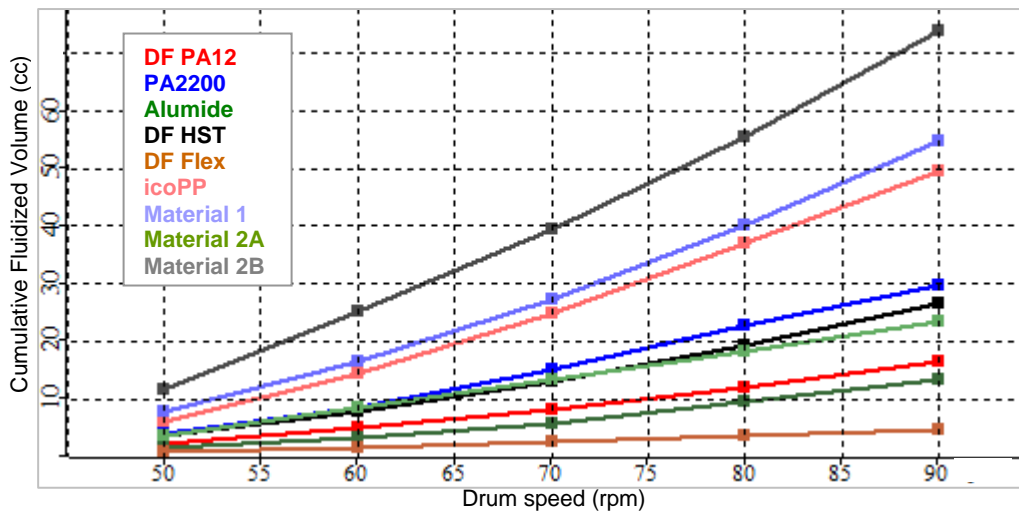
Figure 7: Cumulative Fluidized Height

Figure 8: Cumulative Fluidized Volume

Both figures depict a linear correlation between the drum speed from 50 to 90 rpm and the fluidized height and volume. As noted, materials with a finer PSD and near spherical shape present the maximum volume slopes. For the fluidized height the same trend is observed. It must be pointed out that the term "fluidized" refers specifically to a powder that presents a bulk volume expansion due the entrapped air or gas during powder agitation when the fluid evacuates the powder interstices at a lower rate than the fluid that is introduced inside the inter-particle voids. However, this condition might not be necessary to achieve a volume expansion. Thus, it must be distinguished between the effect of a real fluidization or just a volume dilatation due the reduction of the coordination number when particles move in a shear displacement relative to each other. This phenomenon is known as dilatancy[1] [32]. This effect can be analysed by the Final Settling Time parameter. If after the drum detention this value turns out to be negligible, it indicates that the particles remain in contact due their interconnections and the powder does not really fluidize.
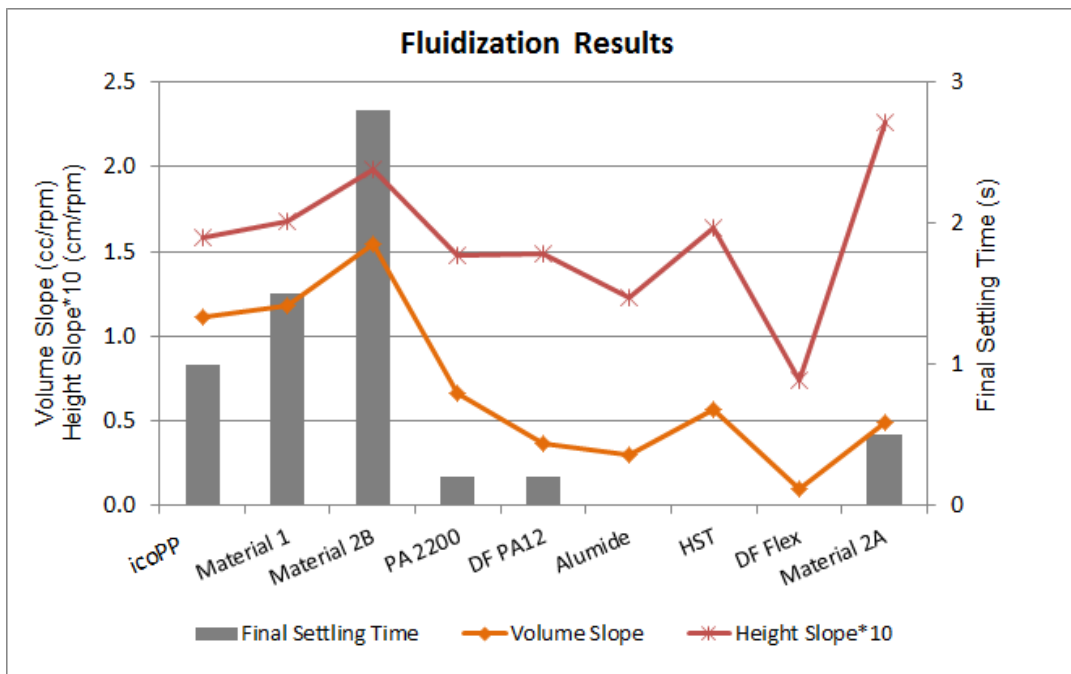

Figure 9: Summary of results for Fluidization Indexes

Analysing the results depicted in Figure 9, it can be observed that the first three materials present the highest settling times coupled with the maximum height and volume slopes. It can be stated that these powders develop a fluidized state. DF PA12 and PA 2200 depict lower settling time values correlated to an incipient fluidization. On the other hand, both filled materials with heterogeneous phases (Alumide & DF HST) and DF Flex clearly show a dilatancy effect with lower volume expansion rates. DF Flex seems even to be invariant to the drum rotational speed. This can explain why it presents a lower VER value as the bulk volume remains almost unchanged from its compacted condition (tap density). In case of Material 2A a particular condition occurs. The powder partially fluidizes with a lower volume expansion rate and a higher

---

[1] For the Fluidization test its name is used indistinctively for any of both conditions, i.e., a real fluidization or dilatancy

height slope. From the flowability results, this powder presents the maximum VER value. This indicates that the powder easily reaches a low bulk density (high expanded volume) from its initial compacted condition (tap density) under slow rotational speeds. That can be achieved only due a dilatancy effect. Therefore, this material, due to its particle flake shape, increases its height just at the top free surface due the avalanching effect coupled to a high interlocking between particles, but without increasing the fluidized volume width[2], which remains quite similar to DF PA12 (see Table 4).

Concerning the SLS powder deposition, a distinction between fluidization and dilatancy could predict to a certain extent how the deposition speed can affect the packing conditions. If the powder presents a higher fluidization rate like Material 2B, a higher speed will lead to a poor packing state. Thus, a lower translational velocity of the spreading system must be considered. On the other hand, if the powder density condition is less sensitive to this variable, a relative constant packing will be obtained. However, if a strong dilatancy effect is present, like for Material 2A, a lower part bed density can also be obtained.

5 Summary

A new SLS powder characterization methodology has been introduced considering the dynamic tumbling behavior under a similar processing stress state when the powder is mechanically agitated inside a rotational drum. The Revolution Powder Analyzer system was employed and different characterization indexes were described and correlated to the SLS process.

Different commercial powders and others under research were analyzed. New aspects regarding powder rearrangement were coupled to traditional measurement indexes to improve the description of the powder packing performance. Thus, a new characterization indicator is proposed, which could help to rank more accurately newly developed powders, assessing a sensitive differentiation.

The intent is not to replace traditional methods, but complement those existent to achieve a more accurate understanding about SLS powder suitability and thus reduce the powder development cycle time.

Of course, it must be remarked, that an adequate powder spreading and packing is just one of the fundamental conditions that must be met to successfully sinter a material and even a good flowing powder that presents unsuitable intrinsic properties can be rejected.

Finally, this research was limited to new materials. Powder flowing properties after recycling and the behaviour at the chamber processing temperature are still open inquiries that must be addressed in a further study.

---

[2] The fluidized width is obtained by the ratio between the fluidized volume and the fluidized height and drum depth.

6 References

[1] Schmid, M. and Levy, G. (2009), "Lasersintermaterialien – aktueller Stand und Entwicklungspotential", (eds. D. Rietzel, F. Kühnlein, D. Drummer), Fachtagung Additive Fertigung, Lehrstuhl für Kunststofftechnik, Universität Erlangen, pp. 43-55.

[2] Jain, P.K., Senthilkumaran, K., Pandey, P.M. and Rao, P.V.M. (2006), "Advances in materials for powder based rapid prototyping", In Proceeding of International Conference on Recent Advances in Materials and Processing, Coimbatore, India.

[3] Goodridge, R.D., Tuck, C.J. and Hague, R.J.M. (2011), "Laser Sintering of Polyamides and Other Polymers", Progress in Materials Science, *In Press, Corrected Proof*, Available online 17 May 2011.

[4] Schmidt, M., Pohle, D., and Rechtenwald, T. (2007), "Selective Laser Sintering of PEEK", CIRP Annals - Manufacturing Technology, 56(1), pp. 205-208.

[5] Schmid, M., Amado, F. and Levy, G. (2011), "iCoPP - A New Polyolefin for Additive Manufacturing (SLS)", Proceedings of the International Conference on Additive Manufacturing, Session 7, Loughborough, U.K.

[6] Schultz, J.P. (2003), "Modeling Heat Transfer and Densification during Laser Sintering of Viscoelastic Polymers", Doctoral Dissertation, Virginia Polytechnic Institute and State University, Blacksburg (VA), USA.

[7] Salmoria, G.V., Leite, J.L., Paggi, R.A., Lago, A., Pires, A.T.N. (2008), "Selective laser sintering of PA12/HDPE blends: Effect of components on elastic/plastic behavior", Polymer Testing, 27(6), pp. 654-659.

[8] Schultz, J.P., Martin, J.P., Kander, R. G. and Suchicital, C.T.A. (2000), "Selective Laser Sintering of Nylon 12-PEEK Blends Formed by Cryogenic Mechanical Alloying", Proceedings SFF Symposium, Austin (TX), USA, pp. 119-124.

[9] Pfister, A. (2005), "Neue Materialsysteme für das Dreidimensionale Drucken und das Selektive Lasersintern", Doctoral Dissertation, Albert Ludwigs Universität, Freiburg, Germany.

[10] Salmoria, G.V., Leite, J.L. and Paggi, R.A., (2009), "The microstructural characterization of PA6/PA12 blend specimens fabricated by selective laser sintering", Polymer Testing, 28(7), pp. 746-751.

[11] Koo, J.H., Lao, S., Ho, W., Ngyuen, K., Cheng, J., Pilato, L., Wissler, G. and Ervin, M. (2006), "Polyamide Nanocomposites for Selective Laser Sintering", Proceedings SFF Symposium, Austin (TX), USA, pp. 392-409.

[12] Shi, Y., Wang, Y., Chen, J. and Huang, S. (2008), "Experimental investigation into the selective laser sintering of high-impact polystyrene", Journal of Applied Polymer Science, 108(1), pp. 535-540.

[13] Gill, T. and Hon, B. (2002), "Selective Laser Sintering of SiC/Polyamide Matrix Composites", Proceedings SFF Symposium, Austin (TX), USA, pp. 538-545.

[14] Hon, K.K.B., Gill, T.J. (2003), "Selective Laser Sintering of SiC/Polyamide Composites", CIRP Annals - Manufacturing Technology, 52(1), pp. 173-176.

[15] Berti, G., D'Angelo, L., Gatto, A. and Iuliano, L. (2010), "Mechanical characterisation of PA-Al2O3 composites obtained by selective laser sintering", Rapid Prototyping Journal, 16(2), pp. 124-129.

[16] Salmoria, G.V., Paggi, R.A., Lago, A. and Beal, V.E. (2011), "Microstructural and mechanical characterization of PA12/MWCNTs nanocomposite manufactured by selective laser sintering", Polymer Testing, 30(6), pp. 611-615.

[17]   Athreya, S.R., Kalaitzidou, K. and Das, S. (2010), "Processing and characterization of a carbon black-filled electrically conductive Nylon-12 nanocomposite produced by selective laser sintering", Materials Science and Engineering: A, 527(10-11), pp. 2637-2642.

[18] Wahab, M.S., Dalgarno, K.W., Cochrane, R.F. and Hassan, S. (2009), "Development of Polymer Nanocomposites for Rapid Prototyping Process", Proceedings of the World Congress on Engineering WCE, Vol II, London, U.K.

[19] Kim, J. and Creasy, T.S. (2004), "Selective laser sintering characteristics of nylon 6/clay-reinforced nanocomposite", Polymer Testing, 23(6), pp. 629-636.

[20] Cheng, J., Lao, S., Nguyen, K., Ho, W., Cummings, A. and Koo, J. (2005), "SLS Processing Studies of Nylon 11 Nanocomposites", Proceedings SFF Symposium, Austin (TX), USA, pp. 141-149.

[21] Chunze, Y., Yusheng, S., Jinsong, Y. and Jinhui, L. (2009), "A Nanosilica/Nylon-12 Composite Powder for Selective Laser Sintering", Journal of Reinforced Plastics and Composites, 28(23), pp. 2889-2902.

[22] Yang, J., Shi, Y. and Yan, C. (2010), "Selective laser sintering of polyamide 12/potassium titanium whisker composites", Journal of Applied Polymer Science, 117(4), pp. 2196-2204.

[23] Yan, C.Z., Shi, Y.S., Yang, J.S. and Liu, J.H. (2011) "An organically modified montmorillonite/nylon-12 composite powder for selective laser sintering", Rapid Prototyping Journal, 17(1), pp. 28-36.

[24] Martin, J.P. and Kander, R.G. (2000), "Characterization of Mechanically Alloyed Polymer Blends for Selective Laser Sintering", Proceedings SFF Symposium, Austin (TX), USA, pp. 92-99.

[25] Schulze, D. (2007), *Powders and Bulk Solids: Behavior, Characterization, Storage and Flow*, Springer, 1st Edition, Germany.

[26] Evans, R. S., Bourell, D. L., Beaman, J. J. and Campbell, M.I. (2005), "SLS Materials Development Method for Rapid Manufacturing", Proceedings SFF Symposium, Austin (TX), USA, pp. 184-196.

[27] Krantz, M., Zhang, H. and Zhu, J. (2009), "Characterization of powder flow: Static and dynamic testing", Powder Technology, 196(1), pp. 239-245.

[28] Alscher, G. (2000), "Das Verhalten teilkristalliner Thermoplaste beim Lasersintern", Doctoral Dissertation, Universität GH, Essen, Germany.

[29] Allen, M., Brown, G.J. and Miles, N.J. (1995), "Measurement of boundary fractal dimensions: review of current techniques", Powder Technology, 84, pp. 1-14.

[30] Soh, J., Liew, C. and Heng, P. (2006), " New Indices to Characterize Powder Flow Based on Their Avalanching Behavior", Pharmaceutical Development and Technology, 11(1), pp. 93-102.

[31] Abdullah, E.C. and Geldart, D. (1999), "The use of bulk density measurements as flowability indicators", Powder Technology, 102, pp. 151-165.

[32] Abriak, N.E. and Caron, J.F. (2006), "Experimental study of shear in granular media", Advanced Powder Technology, 17(3), pp. 297-318.